

# Theoretical prediction of ultrasensitive sensing in 3D stochastic interferometry

Guillaume Graciani\*

*SAMOVAR, Télécom SudParis, Institut Polytechnique de Paris, 91120 Palaiseau, France*

Marcel Filoche

*Institut Langevin, ESPCI Paris, PSL University, CNRS, 75005 Paris, France*

We show that a random light field can be used for high-precision metrology purposes, given the introduction of specific boundary conditions in the form of Lambertian reflections inside a cavity. We demonstrate a quantifiable and reproducible interferometric response to minute perturbations in wavelength, refractive index, and geometry, predicting high sensitivities in good agreement with experimental measurements of geometrical deformations down to the picometer.

Speckle metrology consists in harvesting the seemingly random interference pattern formed by a beam of coherent light going through a complex medium to study the properties of either the light, or of its supporting medium: ultra-sensitive wavelength determination and spectral analysis [1, 2], refractive index sensing [3], small angles and displacements metrology [4], or the well-known Dynamic Light Scattering (DLS) [5] and Diffusing Wave Spectroscopy (DWS) [6–9] for particle sizing and rheology [10, 11] to name a few.

While in most of these applications, the very speckle pattern used for metrology is directly generated from the medium under study, we propose here a fundamentally different interferometric approach in which a 3D field of random waves is independently generated inside a cavity and used to measure perturbations acting upon it. This setup maximizes sensitivity through laser resonance phenomena, at the expense of any spatial information on the perturbation. This paper finds support in our recent realization of such a so-called 3D stochastic interferometer, used as a highly sensitive way to homogeneously probe the geometric and dielectric fluctuations of an optical volume [12, 13], seismic and acoustic vibrations [13], amplify Dynamic Light Scattering for particle sizing [14], and perform a marker-free study of protein dynamics in solution [15]. In this paper, we theoretically derive the high sensitivity of this setup to perturbations of the medium, and numerically compute noise floors in excellent agreement with experimental realizations.

## Experimental realization

The experimental setup consists in a single-frequency laser propagating inside a closed, high-reflectivity Lambertian cavity, and a light detection scheme capable of probing the speckle field within it. The randomness and the high statistical symmetry of the optical field arise from the linear transformation of the input laser field by the extreme—but deterministic—complexity of multiple scattering due to the quenched disorder of the Lambertian wall structure. This highly complex boundary condition acts as a feedback that leads to the interferometric properties of the field.

Each point inside the cavity corresponds to the coherent superposition of a very large number of interfering plane waves, leading to a 3D speckle that is stationary unless the geometry of the cavity or the dielectric properties of its content fluctuate. Due to the statistical homogeneity and isotropy of the light field, all points in the cavity, all directions, and all polarization states are statistically equivalent regardless of the geometry of the cavity [12].

It follows a unique property: a phase perturbation can propagate from one point of the cavity to any other point with a random path whose statistical properties do not depend on their positions. As a consequence, the cavity and the field inside can be used as one single interferometer, in the sense that its response depends neither on the cavity shape, nor on how the light is injected, nor on where perturbations take place nor on where the response is measured [12]. When injecting a single-frequency laser at a given input point, each plane wave that is observed at any other location is coupled to the laser field at the input point, and its random phase essentially reflects the phase lag corresponding to the length of the random propagation path that connects the two points, see Fig. 1. In the following, we will consider three types of average for any measured quantity  $X$ :  $\bar{X}$  will denote a spatial average,  $\langle X \rangle_t$  a time average, and  $\langle X \rangle_c$  an average over all speckle configurations, respectively.

Taking into account not only the length of a chord  $\Lambda_c$ , but also the diffusive random walk inside the walls needed for the diffuse reflection process, we get that the total path length of a photon can be represented as a composite random variable:

$$\Lambda = n_c \Lambda_c + n_r c \tau_r, \quad (1)$$

where  $n_r$  is the random number of reflections,  $n_c = n_r + 1$  the number of free-space chords through the cavity, and  $\tau_r$  a random variable that corresponds to the residency duration of the photon inside the wall at each reflection, also called reflection time. Note that the mean chord length within a cavity of volume  $V_c$  and surface  $\Sigma_c$  satisfies the well-known property  $\bar{\Lambda}_c = 4V_c/\Sigma_c$  [12, 16, 17].

The phase  $\phi$  of each plane wave is therefore associated to this optical length  $\Lambda$ , and can be rewritten introducing

the aforementioned average chord length:

$$\phi = \frac{2\pi\Lambda}{\lambda_0} = \frac{2\pi\bar{\Lambda}}{\lambda_0} + \frac{2\pi}{\lambda_0} (\Lambda - \bar{\Lambda}) = \bar{\phi} + k\tilde{\Lambda}, \quad (2)$$

where  $\bar{\phi}$  is the average phase lag and  $k\tilde{\Lambda} = k(\Lambda - \bar{\Lambda})$  is the phase shift specific to each path. In the experimental realization,  $\bar{\Lambda}$  was measured  $\sim 62$  m, about 8 orders of magnitude larger than the laser wavelength  $\lambda_0$  [12]. Assuming that the standard deviation  $\sigma_\Lambda$  is of the same order of magnitude than  $\bar{\Lambda}$ , we can safely assume that the standard deviation  $\sigma_\phi$  of the phases is approximately 8 orders of magnitude larger than  $2\pi$ , and that phases are thus uniformly distributed over  $[0, 2\pi]$ .

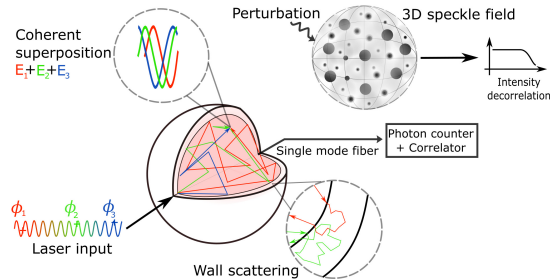


FIG. 1. Schematics of the setup: A monochromatic laser is injected inside a Lambertian cavity. Three light paths of different lengths are represented in blue, green, and red (from shortest to longest), leading to a three-wave superposition and a 3D speckle field. Outside perturbations acting upon it induce intensity decorrelations, probed by a single mode fiber, a photon counter, and a correlator.

### Mathematical structure of the random wave field

A 3D field of random waves can be represented in a purely classical way as the real part  $E(\mathbf{r}, t)$  of a complex vector field  $\mathbf{E}(\mathbf{r}, t)$  in  $\mathbb{C}^3$ , constructed as the coherent sum of a large statistical set of elementary plane waves indexed by  $\alpha \in \mathbb{N}$ . Each elementary wave  $\mathbf{E}_\alpha(\mathbf{r}, t)$  has a complex amplitude  $a_\alpha e^{i\phi_\alpha}$ , and carries a polarization

represented by a complex unitary vector  $\mathbf{d}_\alpha$  perpendicular to  $\mathbf{k}_\alpha$ , the wave vector. This elementary wave reads:

$$\mathbf{E}_\alpha(\mathbf{r}, t) = a_\alpha e^{i\phi_\alpha} \mathbf{d}_\alpha \exp(i\mathbf{k}_\alpha \mathbf{r} - i\omega_\alpha t). \quad (3)$$

The key assumptions made by Berry [18] to construct the 3D random wave model are:

1. Each elementary wave is a random object defined by three independent random variables: a wave vector  $\mathbf{k}_\alpha$ , a phase  $\phi_\alpha$ , and a polarization  $\mathbf{d}_\alpha$ .
2. The random wave vector  $\mathbf{k}_\alpha$  is uniformly distributed on the 3D sphere  $|\mathbf{k}_\alpha| = k = 2\pi/\lambda_0$ ; the phase is uniformly distributed on  $[0, 2\pi]$ ; the polarization state is uniformly distributed on the Poincaré sphere.
3. The total field is a random sum of independent and identically distributed elementary waves.

The amplitudes  $a_\alpha$  are normalization constants defined by the energy density of the field. Each statistical set of random waves  $\{\mathbf{E}_\alpha(\mathbf{r}, t)_{1 \leq \alpha \leq N_C}\}$  is referred to as a microscopic configuration of the field,  $\mathcal{C} = \{(a_\alpha, \mathbf{d}_\alpha, \phi_\alpha, \mathbf{k}_\alpha)_{1 \leq \alpha \leq N_C}\}$ , where  $N_C$  is the number of elementary waves:

$$\mathbf{E}(\mathbf{r}, t, \mathcal{C}) = \sum_{\alpha=1}^{N_C} a_\alpha \mathbf{d}_\alpha e^{i\phi_\alpha} \exp(i\mathbf{k}_\alpha \mathbf{r} - i\omega t). \quad (4)$$

Each such microscopic configuration  $\mathcal{C}$  corresponds to a large number of degrees of freedom equal to the product of  $N_C$  by the number of degrees of freedom of each field component. While there is no mathematical reason to set any particular upper bound to  $N_C$ , the diffraction theory provides an estimate of this bound  $\sim 10^{10}$  (see Appendix A).

Let us now consider a point  $\mathbf{r}$  in the cavity, and the time-averaged optical intensity  $I(\mathbf{r}, \mathcal{C}) = c\epsilon_0 \langle E^2(\mathbf{r}, t, \mathcal{C}) \rangle_t$  of the real field  $E(\mathbf{r}, t, \mathcal{C}) = \mathcal{R}e(\mathbf{E}(\mathbf{r}, t, \mathcal{C}))$  for a microscopic configuration  $\mathcal{C}$ . Using the complex vector formalism, it comes:

$$I(\mathbf{r}, \mathcal{C}) = c\epsilon_0 \langle \mathbf{E}(\mathbf{r}, t, \mathcal{C}) \mathbf{E}^*(\mathbf{r}, t, \mathcal{C}) \rangle_t = \frac{c\epsilon_0}{2} \left[ \sum_{\alpha=1}^{N_C} a_\alpha \mathbf{d}_\alpha e^{i\phi_\alpha} e^{i\mathbf{k}_\alpha \mathbf{r}} \right] \left[ \sum_{\beta=1}^{N_C} a_\beta \mathbf{d}_\beta e^{i\phi_\beta} e^{i\mathbf{k}_\beta \mathbf{r}} \right]^*. \quad (5)$$

For a given configuration  $\mathcal{C}$ , the field complex amplitude obeys a zero-mean circular complex Gaussian density, and the speckle intensity is therefore exponentially distributed, as expected from a fully developed speckle. The field being fully polarized, it has a unity contrast,

i.e., the standard deviation across space equals the spatial mean [19]:

$$\sigma_{I(\mathbf{r})} | \mathbf{r} = \langle (I(\mathbf{r}, \mathcal{C}) - I(\mathbf{r}', \mathcal{C}))^2 \rangle_{(\mathbf{r}, \mathbf{r}')} = \langle I(\mathbf{r}, \mathcal{C}) \rangle_{\mathbf{r}}. \quad (6)$$

These properties also apply in a dual way to the statis-

tical distribution of the field and the intensity at a given point  $\mathbf{r}$  across the microscopic configurations  $\{\mathcal{C}\}$ , with an exponential distribution of the intensity and a unity contrast, i.e.,  $\sigma_{I(\mathbf{r})|\mathcal{C}} = \langle I(\mathbf{r}) \rangle_{\mathcal{C}}$ .

We also find that the mean intensity at a given point  $\mathbf{r}$  over all microscopic configurations,  $\langle I(\mathbf{r}) \rangle_{\mathcal{C}}$ , does not

depend on  $\mathbf{r}$ , and is equal to the mean intensity for a given configuration across space (showing an ergodicity property of our setup):

$$\langle I(\mathbf{r}, \mathcal{C}) \rangle_{\mathcal{C}} = \langle I(\mathbf{r}, \mathcal{C}) \rangle_{\mathbf{r}} = \bar{I}. \quad (7)$$

It can be factorized using the phase statistics in Eq. (2):

$$\langle I(\mathbf{r}, \mathcal{C}) \rangle_{\mathcal{C}} = \frac{c\epsilon_0}{2} \sum_{1 \leq \alpha, \beta \leq N_{\mathcal{C}}} \langle \mathbf{d}_{\alpha} \mathbf{d}_{\beta}^* \rangle_{\mathcal{C}} \langle e^{i(\mathbf{k}_{\alpha} - \mathbf{k}_{\beta})\mathbf{r}} \rangle_{\mathcal{C}} \langle a_{\alpha} a_{\beta} e^{ik(\tilde{\Lambda}_{\alpha} - \tilde{\Lambda}_{\beta})} \rangle_{\mathcal{C}} = \frac{c\epsilon_0 N_{\mathcal{C}}}{2} \langle a^2 \rangle_{\mathcal{C}}. \quad (8)$$

This simple result requires assumptions satisfied by the random field created in the 3D stochastic interferometer (see Appendix A).

### Interferometric response of the 3D speckle field

In our study, we only consider the perturbation of phase transport and disregard the first-order effects on the geometry of the elementary components of the field, i.e., the polarization  $\mathbf{d}_{\alpha}$  and the direction  $\mathbf{k}_{\alpha}/|\mathbf{k}_{\alpha}|$ . We essentially present a stochastic scalar perturbation theory that extends the well-known theory for classical two-arm interferometers to the case of a random number of isotropically distributed arms with random lengths. Furthermore, we are aware that two metrics are commonly used for quantifying the intrinsic sensitivity of a speckle pattern, namely the spectral correlation function and the similarity [20]. However, those metrics apply to measured 2D images of speckle patterns, while in the present case we will derive an intrinsic sensitivity from the more general Berry formalism. Moreover, this calculation is better suited to a temporal measurement made on a single speckle grain through a monomode fiber, for a frequency analysis, as we have done in [14].

### Wavelength derivative of the speckle intensity

Let us consider a microscopic configuration  $\mathcal{C}$  of the random wave field, associated with the set of path lengths  $\{\Lambda_{\alpha}\}_{\mathcal{C}}$ , and compute the derivative  $\partial_k I(\mathbf{r}, \mathcal{C})$  of the intensity with respect to the wave number of the laser,  $k = 2\pi/\lambda_0$ :

$$\partial_k I(\mathbf{r}, \mathcal{C}) = \frac{c\epsilon_0}{2} \sum_{1 \leq \alpha, \beta \leq N_{\mathcal{C}}} \left[ a_{\alpha} a_{\beta} \mathbf{d}_{\alpha} \mathbf{d}_{\beta}^* e^{ik(\tilde{\Lambda}_{\alpha} - \tilde{\Lambda}_{\beta})} e^{i(\mathbf{k}_{\alpha} - \mathbf{k}_{\beta})\mathbf{r}} \times \left[ i(\tilde{\Lambda}_{\alpha} - \tilde{\Lambda}_{\beta}) + i(\mathbf{k}_{\alpha} - \mathbf{k}_{\beta})\mathbf{r}/k \right] \right]. \quad (9)$$

Equation (9) can be interpreted with a thought exper-

iment in which the wave vector of the input light changes from  $k$  to  $k + \delta k$ . The first-order effect of that change on the intensity is given by  $\delta I(\mathbf{r}, \mathcal{C}) = \delta k \cdot \partial_k I(\mathbf{r}, \mathcal{C})$ . A comparison can be made here with a classical 2-arms interferometer, in which the output intensity is not perturbed by  $\delta k$  if its two arms have the same length. However, if the two arms have a known length difference  $\Delta L$ , the perturbation  $\delta k$  can be computed from its deterministic consequence  $\delta I$ . Here instead, each configuration contains a large number of arms, and the interference results from an even larger number of arm pairs  $(\alpha, \beta)$ , which individually come with a random length difference  $(\tilde{\Lambda}_{\alpha} - \tilde{\Lambda}_{\beta})$ . As a result, diagonal terms in Eq. (9) vanish, but non-diagonal terms do not, and they contribute to a non-zero random response characterized by  $\partial_k I(\mathbf{r}, \mathcal{C})$ . However, because the non-diagonal terms  $(\tilde{\Lambda}_{\alpha} - \tilde{\Lambda}_{\beta})$  and  $(\mathbf{k}_{\alpha} - \mathbf{k}_{\beta})$  have zero expectation, the average response vanishes too, i.e.,  $\langle \partial_k I(\mathbf{r}, \mathcal{C}) \rangle_{\mathcal{C}} = 0$ .

Therefore, our setup behaves as a stochastic interferometer, meaning that it responds to a given perturbation  $\delta k$  by a stochastic response  $\delta I(\mathbf{r}, \mathcal{C}) = \delta k \cdot \partial_k I(\mathbf{r}, \mathcal{C})$ , which is a random variable of zero mean. In some way, this is what would happen with a classical two-arm interferometer in which the phase difference  $\varphi_{1,2}$  is a uniform random variable in  $[0, 2\pi]$ . Since the sensitivity  $\partial_{\varphi} I$  for a given phase difference is proportional to  $\sin(\varphi_{1,2})$ , it would then average out to zero over all configurations. Practically, no information can be extracted from using that interferometer with a single configuration, and no information can be obtained from the average response over a large number of configurations either.

The meaningful response is the quadratic response averaged over all microscopic configurations  $\mathcal{C}$ , as defined by:

$$\langle \delta I(\mathbf{r}, \mathcal{C})^2 \rangle_{\mathcal{C}} = \delta k^2 \cdot \langle |\partial_k I(\mathbf{r}, \mathcal{C})|^2 \rangle_{\mathcal{C}}. \quad (10)$$

By introducing  $M_{\alpha, \beta} = i(\tilde{\Lambda}_{\alpha} - \tilde{\Lambda}_{\beta}) + i(\mathbf{k}_{\alpha} - \mathbf{k}_{\beta})\mathbf{r}/k$ , square modulus of Eq. (9) reads:

$$|\partial_k I(\mathbf{r}, \mathcal{C})|^2 = \left[ \frac{c\epsilon_0}{2} \right]^2 \sum_{1 \leq \alpha, \beta, \gamma, \delta \leq N_C} a_\alpha a_\beta a_\gamma a_\delta \mathbf{d}_\alpha \mathbf{d}_\beta^* \mathbf{d}_\gamma^* \mathbf{d}_\delta e^{ik[(\bar{\Lambda}_\alpha - \bar{\Lambda}_\beta) - (\bar{\Lambda}_\gamma - \bar{\Lambda}_\delta)]} e^{i(\mathbf{k}_\alpha - \mathbf{k}_\beta)\mathbf{r}} e^{-i(\mathbf{k}_\gamma - \mathbf{k}_\delta)\mathbf{r}} M_{\alpha, \beta} M_{\gamma, \delta}^*. \quad (11)$$

We now average this equation over all configurations, which amounts to considering the average for a random set of 4 waves  $\langle \dots \rangle_{(\alpha, \beta, \gamma, \delta)}$ . The average over non-diagonal pairs of waves vanishes, i.e.,  $\langle \dots \rangle_{(\alpha, \beta) \neq (\gamma, \delta)} = 0$ , and only the diagonal terms corresponding to  $(\alpha, \beta) = (\gamma, \delta)$  remain. For these diagonal pairs, the contribution of polarization vectors is 1 because they are unitary. Moreover, pairs  $\alpha = \beta$  do not contribute as seen above in the analogy with equal arms interferometers.

We are left with computing the average  $\langle a_\alpha^2 a_\beta^2 |M_{\alpha, \beta}|^2 \rangle_{\alpha \neq \beta}$ . Because variables  $\tilde{\Lambda}$  and  $\mathbf{k}$  are independent, and since  $\langle \mathbf{k}_\alpha \mathbf{k}_\beta \rangle_{\alpha \neq \beta} = \langle \mathbf{k}_\alpha \rangle \langle \mathbf{k}_\beta \rangle_{\alpha \neq \beta} = 0$ , it comes (see Appendix B for the detailed derivation):

$$\langle |\partial_k I(\mathbf{r}, \mathcal{C})|^2 \rangle_{\mathcal{C}} = N_C(N_C - 1) \frac{c^2 \epsilon_0^2}{2} \left[ \langle a^2 \rangle \langle a^2 \tilde{\Lambda}^2 \rangle - \langle a^2 \tilde{\Lambda} \rangle^2 \right]. \quad (12)$$

We observe that the statistics of the mean-square sensitivity are independent of  $\mathbf{r}$ . From now on, we will omit the spatial variable  $\mathbf{r}$  and consider a fixed arbitrary position  $\mathbf{r} = 0$ . Assuming that the field amplitude  $a$  and the path length  $\Lambda$  are independent variables, considering that  $N_C \gg 1$ , and using the normalization of the intensity from Eq. (8), we find:

$$\langle |\partial_k I|^2 \rangle_{\mathcal{C}} = 2 \langle I \rangle_{\mathcal{C}}^2 \sigma_{\tilde{\Lambda}}^2, \quad (13)$$

where  $\sigma_{\tilde{\Lambda}}^2 = \sigma_{\Lambda}^2$  is the variance of the path length distribution  $\tilde{\Lambda}$ . From Eq. (1), we see that the exact value of the variance  $\sigma_{\tilde{\Lambda}}^2$  requires the knowledge of variances  $\sigma_{n_r}^2$ ,  $\sigma_{\Lambda_c}^2$  and  $\sigma_{\tau_r}^2$ , of  $n_r$ ,  $\Lambda_c$ , and  $\tau_r$ , respectively. We find:

$$\sigma_{\tilde{\Lambda}}^2 = G^2 \left[ \bar{\Lambda}_c^2 + 2\sigma_{\Lambda_c}^2 + c^2 \bar{\tau}_r^2 + 2c^2 \sigma_{\tau_r}^2 \right], \quad (14)$$

where  $G = -1/\ln(\rho)$  is the cavity gain and  $\rho$  its albedo.

Practically in our experiments, the size of the cavity is large enough for the contribution of  $c\tau_r$  to be negligible compared to  $\Lambda_c$ , and the variance of  $\Lambda$  can be safely approximated accordingly, leading to  $\sigma_{\tilde{\Lambda}}^2 \approx \sigma_{n_r \Lambda_c}^2 = G^2 [\bar{\Lambda}_c^2 + 2\sigma_{\Lambda_c}^2]$ . Using the ergodicity property  $\langle I \rangle_{\mathcal{C}} = \bar{I}$  found in Eq. (7), it comes:

$$\langle |\partial_k I|^2 \rangle_{\mathcal{C}} = 2 (G \bar{\Lambda}_c \bar{I})^2 \left( 1 + 2 \frac{\sigma_{\Lambda_c}^2}{\bar{\Lambda}_c^2} \right). \quad (15)$$

In addition, the response to small variations of the wavelength is given by the derivative  $\partial_\lambda I = -(k/\lambda) \partial_k I$ :

$$\langle |\partial_\lambda I|^2 \rangle_{\mathcal{C}} = 2 (G k \bar{\Lambda}_c \bar{I} / \lambda)^2 \left( 1 + 2 \frac{\sigma_{\Lambda_c}^2}{\bar{\Lambda}_c^2} \right). \quad (16)$$

---

### Derivative with respect to the cavity geometry

Our experimental results show that the speckle intensity is sensitive to deformations of the cavity of the order of a few picometers under the conditions described in [14]. Similarly to the previous calculation, we show (see Appendix C) that the response to small variations of the cavity geometry (defined by a linear scaling parameter  $\mu$ ) is given by:

$$\langle |\partial_\mu I|^2 \rangle_{\mathcal{C}} = 2 (G k \bar{\Lambda}_c \bar{I})^2 \left( 1 + 2 \frac{\sigma_{\Lambda_c}^2}{\bar{\Lambda}_c^2} \right). \quad (17)$$

An analogous formula can also be obtained when considering a spatial variation the refractive index  $n = n_0 + \delta n$  of the cavity medium.

### Experimental sensitivity

In this section, we generalize the theoretical approach used in the previous sections to derive an expression for the sensitivity of the instrument with respect to any perturbation of the field (wavelength, cavity size, refractive index, or any quantity for which we can compute the partial derivative of the speckle intensity). We then numerically calculate the noise floor with experimental parameters, only to derive an expression in terms of a temporal decorrelation function.

Let us consider an experiment in which a measured intensity  $I(\mathcal{C})$  is obtained from a microscopic configuration  $\mathcal{C}$  of the speckle, and a perturbation  $\delta p$  applied to one parameter  $p$  of the field. The variation of the intensity  $\delta I = I(\mathcal{C}_{p+\delta p}) - I(\mathcal{C}_p)$  is given at first order by  $\delta I \approx \delta p \cdot \partial_p I(\mathcal{C})$ .  $\delta I$  can therefore be seen as a random variable indexed on the set of field configurations  $\{\mathcal{C}\}$ . As discussed in the previous section, the meaningful quantity is the mean-square variation over  $\{\mathcal{C}\}$  which reads  $\langle \delta I^2 \rangle_{\mathcal{C}} = \delta p^2 \cdot \langle |\partial_p I|^2 \rangle_{\mathcal{C}}$ .

The interferometric sensitivity  $S_p$  to variations of the parameter  $p$  can be generically defined as the ratio of the relative root-mean square (*rms*) intensity variations over the perturbation  $|\delta p|$ . The so-called *rms* sensitivity comes as:

$$S_p = \frac{\sqrt{\langle \delta I_{(\delta p)}^2 \rangle_{\mathcal{C}}}}{|\delta p| \bar{I}} = \frac{\sqrt{\langle |\partial_p I|^2 \rangle_{\mathcal{C}}}}{\bar{I}}. \quad (18)$$

Using Eqs (16)-(17), we obtain the *rms* sensitivities  $S_\lambda$ ,  $S_n$  or  $S_\mu$  to changes of the wavelength, the index of re-

fraction, or the scaling parameter  $\mu$ :

$$S_p = 2\sqrt{2}\pi G \bar{\Lambda}_c \lambda^{-\alpha} \sqrt{1 + 2 \frac{\sigma_{\bar{\Lambda}_c}^2}{\bar{\Lambda}_c^2}} \approx 10 G \frac{\bar{\Lambda}_c}{\lambda^\alpha}, \quad (19)$$

where the exponent  $\alpha$  is 2 for a wavelength perturbation, and 1 for a deformation or a change in the refractive index. Practically, for the cavity used in previous publications [12]:

$$\frac{\sqrt{\langle \delta I_{(\delta p)}^2 \rangle_C}}{\bar{I}} = \begin{cases} 1.4 \times 10^{15} |\delta \lambda| \\ 9.4 \times 10^8 |\delta n| \\ 9.4 \times 10^8 |\delta \mu| \end{cases}. \quad (20)$$

Measuring the intensity subjected to a perturbation  $\delta p$  with  $n_{ph}$  photons, the previous equation gives the signal to noise ratio (SNR) associated to the intensity:

$$|\delta p|_{\min} = \frac{\lambda^\alpha}{2\pi G \bar{\Lambda}_c} \frac{\text{SNR}}{\sqrt{n_{ph}}}. \quad (21)$$

As a result, with  $n_{ph} = 10^6$  photons, e.g., with a 100 kHz counting rate during 10s, and  $\text{SNR} \geq 10$ , we get  $|\delta \lambda| \geq 1.1 \times 10^{-17}$  m or  $|\delta n| \geq 1.7 \times 10^{-11}$  which are in good agreement with experimental realizations of other teams [21, 22]. The detection limit  $|\delta \lambda|_{\min} \approx 10^{-17}$  m can be used to estimate the sensitivity to cavity deformations in our experiment. Using the relation  $|\delta \bar{\Lambda}_c|/\bar{\Lambda}_c = |\delta \lambda|/\lambda$ , we find a theoretical picometer level sensitivity  $|\delta \bar{\Lambda}_c|_{\min} \approx 10^{-12}$  m, in excellent agreement with our experimental measurements, about  $2.7 \times 10^{-12}$  m [12].

### Conclusion

In summary, we have shown that a superposition of coherent and random light waves provides a deterministic and quantifiable intensity response to an outside perturbation, be it a change in wavelength or refractive index.

We derived the theoretical expected sensitivity of such instruments to external perturbations, including changes in the instrument geometry, that can access the picometer scale. This level of performance has been demonstrated in experimental realizations of Lambertian cavities, which act as so-called 3D stochastic interferometers.

Even if such intrinsically random fields have been extensively described after their first introduction by Berry [23–26], it has been so mostly within the framework of geometry and topology, with a focus on optical vortices and phase singularities [27], and very few direct experimental realizations within that context [28–30]. The essence of the interferometric response that we describe lies in the boundary conditions brought by Lambertian cavity walls, which introduce feedback as opposed to the boundless conditions used in Berry’s theoretical description. Mostly used for high precision photometry [31, 32] and occasionally coherent applications [21], we bring those cavities under the new light of the random wave model, bridging the gap between random light fields and interferometry.

3D stochastic interferometry has applications ranging from particle sizing, rheology, marker-free protein study, to even vibration sensing, and the theoretical foundation that we present in this study proves that it can be efficiently used to design high-sensitivity experiments. In addition, the field of random waves has been shown to raise deep fundamental questions in quantum mechanics or even superfluids, and this current study could shed new light on these phenomena, given its original experimental approach to the subject.

### ACKNOWLEDGMENTS

The authors are grateful to Profs. François Amblard, John King, Joerg Enderlein, Philippe Poulin, Shankar Ghosh and Rodney Ruoff for comments and discussions. This work has been supported by a grant from the Simons Foundation (Grant No. 601944).

- 
- [1] Y. Wan, X. Fan, and Z. He, Review on speckle-based spectrum analyzer, *Photonic Sensors* **11**, 187 (2021).
  - [2] N. K. Metzger, R. Spesyvtsev, G. D. Bruce, B. Miller, G. T. Maker, G. Malcolm, M. Mazilu, and K. Dholakia, Harnessing speckle for a sub-femtometre resolved broadband wavemeter and laser stabilization, *Nat. Commun.* **8**, 15610 (2017).
  - [3] V. Tran, S. K. Sahoo, D. Wang, and C. Dang, Utilizing multiple scattering effect for highly sensitive optical refractive index sensing, *Sens. Actuator A-Phys.* **301**, 111776 (2020).
  - [4] A. Vijayakumar, D. Jayavel, M. Muthaiah, S. Bhattacharya, and J. Rosen, Implementation of a speckle-correlation-based optical lever with extended dynamic range, *Appl. Opt.* **58**, 5982 (2019).
  - [5] B. J. Berne and R. Pecora, *Dynamic light scattering: with applications to chem...* (Courier Corporation, 2000).
  - [6] G. Maret and P. E. Wolf, Multiple light scattering from disordered media. the effect of brownian motion of scatterers, *Z. Phys. B Condens. Matter* **65**, 409 (1987).
  - [7] D. J. Pine, D. A. Weitz, P. M. Chaikin, and E. Herbolzheimer, Diffusing wave spectroscopy, *Phys. Rev. Lett.* **60**, 1134 (1988).
  - [8] F. C. MacKintosh and S. John, Diffusing-wave spectroscopy and multiple scattering of light in correlated random media, *Phys. Rev. B* **40**, 2383 (1989).
  - [9] G. Graciani, L. Le Goff, and F. Amblard, Protein conformational dynamics probed correlation spectroscopy of multiply scattered light, *Biophys. J.* **118**, 136a (2020).

- [10] P. Zakharov and F. Scheffold, Advances in dynamic light scattering techniques, in [Light Scattering Reviews 4: Single Light Scattering \[...\]](#), edited by A. A. Kokhanovsky (Springer Berlin Heidelberg, Berlin, Heidelberg, 2009) pp. 433–467.
- [11] H. S. Kim, N. Şenbil, C. Zhang, F. Scheffold, and T. G. Mason, Diffusing wave microrheology of highly scattering concentrated monodisperse emulsions, [Proc. Natl Acad. Sci. USA](#) **116**, 7766 (2019).
- [12] G. Graciani, M. Filoche, and F. Amblard, 3D stochastic interferometer detects picometer deformations and minute dielectric fluctuations of its optical volume, [Commun. Phys.](#) **5**, 239 (2022).
- [13] G. Graciani and F. Amblard, Random dynamic interferometer: cavity amplified speckle spectroscopy using a highly symmetric coherent field created inside a closed Lambertian optical cavity, in [Applied Optical Metrology III](#), Vol. 11102, edited by E. Novak and J. D. Trolinger, International Society for Optics and Photonics (SPIE, 2019) p. 111020N.
- [14] G. Graciani, J. T. King, and F. Amblard, Cavity-amplified scattering spectroscopy reveals the dynamics of proteins and nanoparticles in quasi-transparent and miniature samples, [ACS Nano](#) **16**, 16796 (2022).
- [15] G. Graciani, J. T. King, and F. Amblard, Marker-free protein study by amplified light scattering, in [SPIE Advanced Biophotonics Conference](#), Vol. 12159, edited by E. Chung, K.-H. Jeong, C. Joo, W. Jung, H.-W. Kang, C.-S. Kim, C. Kim, P. Kim, and H. Yoo, International Society for Optics and Photonics (SPIE, 2022) p. 1215908.
- [16] S. Blanco and R. Fournier, Short-path statistics and the diffusion approximation, [Phys. Rev. Lett.](#) **97**, 230604 (2006).
- [17] R. Savo, R. Pierrat, U. Najar, R. Carminati, S. Rotter, and S. Gigan, Observation of mean path length invariance in light-scattering media, [Science](#) **358**, 765 (2017).
- [18] M. V. Berry and M. R. Dennis, Phase singularities in isotropic random waves, [Proc. R. Soc. Lond. A](#) **456**, 2059 (2000).
- [19] J. Uozumi, K. Uno, and T. Asakura, Statistics of gaussian speckles with enhanced fluctuations, [Optical Review](#) **2**, 174 (1995).
- [20] M. Facchin, S. N. Khan, K. Dholakia, and G. D. Bruce, Determining intrinsic sensitivity and the role of multiple scattering in speckle metrology, [Nat. Rev. Phys.](#) **6**, 500 (2024).
- [21] M. Facchin, K. Dholakia, and G. D. Bruce, Wavelength sensitivity of the speckle patterns produced by an integrating sphere, [J. Phys: Photonics](#) **3**, 035005 (2021).
- [22] M. Facchin, G. D. Bruce, and K. Dholakia, Measurement of variations in gas refractive index with  $10^{-9}$  resolution using laser speckle, [ACS Photonics](#) **9**, 830 (2022).
- [23] M. Berry, Chaotic behavior of deterministic systems ed g iooss, rhg helleman and r stora (1983).
- [24] P. O’Connor, J. Gehlen, and E. J. Heller, Properties of random superpositions of plane waves, [Phys. Rev. Lett.](#) **58**, 1296 (1987).
- [25] M. Berry and M. Dennis, Polarization singularities in isotropic random vector waves, [Proc. R. Soc. Lond. A](#) **457**, 141 (2001).
- [26] L. De Angelis, F. Alpeggiani, A. Di Falco, and L. Kuipers, Spatial distribution of phase singularities in optical random vector waves, [Phys. Rev. Lett.](#) **117**, 093901 (2016).
- [27] N. Shvartsman and I. Freund, Vortices in random wave fields: Nearest neighbor anticorrelations, [Phys. Rev. Lett.](#) **72**, 1008 (1994).
- [28] N. Jhajj, I. Larkin, E. W. Rosenthal, S. Zahedpour, J. K. Wahlstrand, and H. M. Milchberg, Spatiotemporal optical vortices, [Phys. Rev. X](#) **6**, 031037 (2016).
- [29] F. Eilenberger, K. Prater, S. Minardi, R. Geiss, U. Röpke, J. Kobelke, K. Schuster, H. Bartelt, S. Nolte, A. Tünnermann, and T. Pertsch, Observation of discrete, vortex light bullets, [Phys. Rev. X](#) **3**, 041031 (2013).
- [30] W. Wang, S. G. Hanson, Y. Miyamoto, and M. Takeda, Experimental investigation of local properties and statistics of optical vortices in random wave fields, [Phys. Rev. Lett.](#) **94**, 103902 (2005).
- [31] I. Khaoua, G. Graciani, A. Kim, and F. Amblard, Stochastic light concentration from 3D to 2D reveals ultraweak chemi- and bioluminescence, [Sci. Rep.](#) **11**, 10050 (2021).
- [32] I. Khaoua, G. Graciani, A. Kim, and F. Amblard, Detectivity optimization to measure ultraweak light fluxes using an em-ccd as binary photon counter array, [Sci. Rep.](#) **11**, 3530 (2021).

## Appendix A: On the mean intensity calculation

Equation (8) in the main text gives an expression for the mean intensity at a given point  $\mathbf{r}$  over all microscopic configurations,  $\langle I(\mathbf{r}) \rangle_{\mathcal{C}}$ . This result requires several assumptions listed in the main text. Here, we remind those assumptions and add their respective justifications:

1. Each configuration  $\mathcal{C}$  refers to a set of independent and identical random variables  $\mathbf{E}_{\alpha}$  indexed by  $\alpha$ .

This issue of independence is directly related to the problem of the numbers of degrees of freedom of the optical field. From diffraction theory, the far-field produced by the cavity walls can be fully represented with a finite set of wave vectors, the size of which is given in order of magnitude by  $\Sigma_c/\lambda^2 \approx 10^{10}$ . As a consequence, for a given configuration  $\mathcal{C}$ , the maximal number of degrees of freedom associated to the corresponding set of wave vectors  $\{\mathbf{k}_{\alpha}\}_{\mathcal{C}}$  has the same order of magnitude. This order of magnitude does not include the degrees of freedom associated with the polarization and the phase, and thus far underestimates the number  $N_{\mathcal{C}}$  of components that need to be considered in the sum. A further discussion would require to also analyze the non-classical degrees of freedom associated with photon numbers. At any rate, the optical field has a finite number of degrees of freedom  $N_{\mathcal{F}}$ , and Eq. (5) provides a meaningful representation of the intensity field if it contains a number of components  $N_{\mathcal{C}} \sim N_{\mathcal{F}}$ . Under this condition, the random variables  $\mathbf{E}_{\alpha}$  entering the representation of the field are independent.

2. The two random vectors variables  $\mathbf{d}$  and  $\mathbf{k}$  are mutually independent variables.

This assumption directly arises from the nature of the diffuse reflection process. As discussed above, this process is deterministic, but its complexity makes it appear as a random process that practically destroys any correlation between the polarization state and the wave vector for any reflected wave.

3.  $\mathbf{d}$  and  $\mathbf{k}$  are independent of the phase and the real amplitude ( $\phi$  and  $a$ ).

For each path  $\alpha$ , the variables  $\mathbf{d}_\alpha$  and  $\mathbf{k}_\alpha$  are determined by the last diffuse reflection event. The phase and the real amplitude instead are determined by the whole stochastic structure of the path, and are therefore independent of  $\mathbf{d}_\alpha$  and  $\mathbf{k}_\alpha$ . They are also mutually independent because of the circular uniformity of the phase.

4. because the polarization is isotropic, non-diagonal terms average to zero.
5.  $\mathbf{d}$  is a unitary variable in  $\mathbb{C}^3$ .

### Appendix B: On the derivation of $\langle |\partial_k I(\mathbf{r}, \mathcal{C})|^2 \rangle_{\mathcal{C}}$

As explained in the main text, only the terms such that  $\alpha \neq \beta$  are left to compute in the sum from Eq. (11), which are as many as  $N_{\mathcal{C}}(N_{\mathcal{C}} - 1)$ . The average  $\langle a_\alpha^2 a_\beta^2 |M_{\alpha,\beta}|^2 \rangle_{\alpha \neq \beta}$  can largely be simplified. Indeed, since  $\langle \mathbf{k}_\alpha \mathbf{k}_\beta \rangle_{\alpha \neq \beta} = \langle \mathbf{k}_\alpha \rangle \langle \mathbf{k}_\beta \rangle_{\alpha \neq \beta} = 0$ , all terms  $k_{\alpha,\beta}^2$  and  $k_\alpha k_\beta$  amount to 0 after averaging. Furthermore, since  $\tilde{\Lambda}$  and  $\mathbf{k}$  are independent, all terms  $\tilde{\Lambda}_{\alpha,\beta} k_{\alpha,\beta}$  also average out to 0. Therefore, the remaining terms to average are  $a_\alpha^2 a_\beta^2 \left[ \tilde{\Lambda}_\alpha^2 + \tilde{\Lambda}_\beta^2 - 2\tilde{\Lambda}_\alpha \tilde{\Lambda}_\beta \right]$ . We then get the following simplification:

$$\langle a_\alpha^2 a_\beta^2 |M_{\alpha,\beta}|^2 \rangle_{\alpha \neq \beta} = 2 \langle a^2 \rangle \langle a^2 \tilde{\Lambda}^2 \rangle - 2 \langle a^2 \tilde{\Lambda} \rangle \langle a^2 \tilde{\Lambda} \rangle, \quad (22)$$

and the final result:

$$\langle |\partial_k I(\mathbf{r}, \mathcal{C})|^2 \rangle_{\mathcal{C}} = N_{\mathcal{C}}(N_{\mathcal{C}} - 1) \frac{c^2 \epsilon_0^2}{2} \left[ \langle a^2 \rangle \langle a^2 \tilde{\Lambda}^2 \rangle - \langle a^2 \tilde{\Lambda} \rangle^2 \right]. \quad (23)$$

### Appendix C: On variations of the intensity due to cavity deformations

To theoretically derive intensity variations from deformations of the cavity is a difficult problem, because there is no mathematical representation of cavity deformations that would be simple enough to derive their effect on the speckle intensity. To circumvent this difficult problem and provide a simplistic but heuristic solution, we use a simple perturbation approach. To represent small cavity deformations that cause a change  $\delta \bar{\Lambda}_c$  of the mean-chord invariant  $\bar{\Lambda}_c = 4V_c/\Sigma_c$ , we introduce the dimensionless scaling parameter  $\mu = 1 + \delta\mu$ , and substitute the random variable  $\Lambda$  that represents random chords by  $\mu\Lambda$ . In this approach, we implicitly assume that the sole effect of  $\delta\mu$  is to induce a phase shift on the elementary fields  $\mathbf{E}_\alpha$ , without changing the geometry of these plane waves.

This strategy relies on the notion that the physics does not change if the scale that measures the wavelength, and the scale that measures the geometry of the cavity down to its smallest microscopic details, are changed by the same factor. By the same token, inasmuch a cavity deformation can be considered to be equivalent to a dilation by the factor  $\mu = 1 + \delta\mu$ , its effect will be equivalent to dilation the wavelength by the factor  $1/\mu$ , i.e., changing the wave vector by the factor  $\mu$ .

With this dimensionless dilation scaling parameter  $\mu$ , the phase factor  $ik(\tilde{\Lambda}_\alpha - \tilde{\Lambda}_\beta)$  is substituted by  $ik\mu(\tilde{\Lambda}_\alpha - \tilde{\Lambda}_\beta)$ , and the speckle intensity can be derived with respect to  $\mu$ . A so-called scale-derivative  $\partial_\mu I = k\partial_k I$  is obtained which reads:

$$\langle |\partial_\mu I|^2 \rangle_{\mathcal{C}} = 2(Gk\bar{\Lambda}_c\bar{I})^2 \left( 1 + 2 \frac{\sigma_{\bar{\Lambda}_c}^2}{\bar{\Lambda}_c^2} \right). \quad (24)$$